Article

Information Dark Energy Can Resolve the Hubble Tension and Is Falsifiable by Experiment

Michael Paul Gough

Department of Engineering and Design, University of Sussex, Brighton BN1 9QT, UK; m.p.gough@sussex.ac.uk

Abstract: We consider the role information energy can play as a source of dark energy. Firstly, we note that if stars and structure had not formed in the universe, elemental bits of information describing the attributes of particles would have exhibited properties similar to the cosmological constant. The Landauer equivalent energy of such elemental bits would be defined in form and value identical to the characteristic energy of the cosmological constant. However, with the formation of stars and structure, stellar heated gas and dust now provide the dominant contribution to information energy with the characteristics of a dynamic, transitional, dark energy. At low redshift, $z < \sim 1.35$, this dark energy emulates the cosmological constant with a near-constant energy density, $w = -1.03 \pm 0.05$, and an energy total similar to the mc^2 of the universe's $\sim 10^{53}$ kg of baryons. At earlier times, $z > \sim 1.35$, information energy was phantom, differing from the cosmological constant, Λ, with a CPL parameter difference of $\Delta w_o = -0.03 \pm 0.05$ and $\Delta w_a = -0.79 \pm 0.08$, values sufficient to account for the H_0 tension. Information dark energy agrees with most phenomena as well as Λ, while exhibiting characteristics that resolve many tensions and problems of ΛCDM: the cosmological constant problem; the cosmological coincidence problem; the H_0 tension, and the σ_8 tension. As this proposed dark energy source is not usually considered, we identify the expected signature in $H(a)$ that will enable the role of information dark energy to be falsified by experimental observation.

Keywords: Landauer's principle; dark energy theory; dark energy experiments

1. Introduction

Many features of the universe are consistent with the standard ΛCDM model. However, as measurements improve in accuracy, a significant difference or tension has been found between the early and late universe Hubble constant, the H_0 values. Planck measurements of the Cosmic Microwave Background, CMB, originating from redshift, z~1100, provide a ΛCDM model-dependent value for today's Hubble Constant, H_0, of 67.4 ± 0.5 km s^{-1} Mpc^{-1} [1]. Independent CMB measurements by the Atacama Cosmology Telescope [2] support Planck with a H_0 value of 67.9 ± 1.5 km s^{-1} Mpc^{-1}. These values are also consistent with those derived from Baryon Acoustic Oscillations [3].

In contrast to these early universe measurements, H_0 measured in the late universe by a wide variety of techniques yields values closer to 73 km s^{-1} Mpc^{-1}. 'Standard candles', provided by type 1a supernovae and Cepheid variable stars, offer distance ladders that yield a value of 74.03 ± 1.42 km s^{-1} Mpc^{-1} [4,5]. A recent comprehensive analysis has further confined the value to 73.04 ± 1.04 km s^{-1} Mpc^{-1} [6]. Other methods have been devised to be independent of standard candle/distance ladder techniques. For example, time delay measurements of multiple-imaged quasars due to strong gravitational lensing [7] provide a value of $73.3 + 1.7/-1.8$ km s^{-1} Mpc^{-1}, differing by 5.3σ from the early universe values. Moreover, the size of edge-on galaxy discs have been determined by the geometry of water maser action occurring in those discs [8], yielding 73.9 ± 3 km s^{-1} Mpc^{-1}, a value greater than the early universe value with a 95–99% level of confidence. Another technique using measurements of infrared surface brightness fluctuation distances in galaxies [9] provides a value of 73.3 ± 2.4 km s^{-1} Mpc^{-1}, again consistent with other late universe values.

Initially, it was thought that this H_0 tension between the early and late universe might be due to systematic errors [10], but over the last couple of years, the many late universe measurements have become more precise and consistent. The persisting H_0 tension implies a problem or tension with the ΛCDM model, even suggesting new physics beyond ΛCDM [4,11,12]. Possible causes of tension include: a late dynamic dark energy; a universe with non-zero curvature; dark matter interaction; an early dark energy; and additional relativistic particles. Natural theoretical values for the cosmological constant, Λ, differ by several orders of magnitude from the value required to explain accelerating expansion. A likely solution to the tension might then be achieved by replacing Λ with a time-dependent dark energy that has a present energy density compatible with the acceleration.

In this paper, we revisit the role of information energy as the source of such dynamic dark energy [13]. Section 2 reviews the expected present information energy density. Section 3 updates previous work with the latest stellar mass density measurements to determine the equation of state parameters. Section 4 shows that the earlier phantom period can quantitatively account for the observed H_0 tension. Section 5 identifies future measurements necessary to confirm or refute this proposed source of dark energy. The discussion in Section 6 shows that information energy could also resolve the cosmological constant problem and the cosmological coincidence problem.

2. Information Energy as Dark Energy

Landauer's Principle provides an equivalent energy for each bit of information or bit of entropy. Landauer showed that information is physical since the erasure of a bit of information in a system at temperature, T, results in the release of a minimum $k_B T \ln(2)$ of energy to the system's surroundings [14,15]. Landauer's principle has now been experimentally verified for both classical bits and quantum qubits [16–19].

A foundational principle has been proposed by Zeilinger [20], whereby the attributes of all particles can be considered at their most basic level as elemental systems with an information content of one bit or qubit. There is a strong similarity between the information energy of such an elemental bit in the universe and the characteristic energy of the cosmological constant [21]. Today, our universe is dominated by dark energy and all matter (baryon + dark), approximately at the ratio of 2:1. If there was no star formation, a representative temperature for matter could be considered to be provided by the temperature, T_u, of a radiation component with the same energy density as all matter:

$$\alpha \, T_u{}^4 = \rho_{tot} \, c^2 \tag{1}$$

where the radiation density constant $\alpha = 4\sigma_{SB}/c$, σ_{SB} is the Stefan–Boltzmann constant, and ρ_{tot} is our universe's total matter density (baryon+dark). σ_{SB} is further defined in terms of fundamental constants:

$$\sigma_{SB} = \pi^2 \, k_B{}^4 / 60 \, \hbar^3 \, c^2 \tag{2}$$

Then, we obtain the Landauer equivalent energy of an elemental bit of information in a universe at temperature T_u:

$$k_B \, T_u \ln(2) = (15 \, \rho_{tot} \, \hbar^3 \, c^5 / \pi^2)^{\frac{1}{4}} \ln(2) \tag{3}$$

This Landauer bit energy is defined identically to the characteristic energy of the cosmological constant. The right-hand side of Equation (3) is identical to Equation 17.14 of [22] for the characteristic energy of the cosmological constant—with the sole addition of ln(2) to convert between entropy units—between natural information units, nats, and bits. Information bit energy might then explain the low milli-eV characteristic energy of Λ, which Peebles [22] considered to be 'too low to be associated with any relevant particle physics'.

Clearly, the universe is not a simple, single system, and here, we follow a phenomenological approach, taking into account star formation and other information energy contributions. Table 1 lists various astrophysical phenomena, their estimated information bit

numbers [23,24], typical temperatures, equivalent information energy total, and that total information energy relative to the universe's total baryon, mc^2.

Table 1. Present information, temperature, and information energy contributions.

|	Information, N, Bits	Typical Temperature T, °K	Information Energy N k_B T ln2, Joules	Information Energy/ Universe Baryon mc^2
Stellar heated gas and dust	$\sim 10^{86}$	$\sim 10^7$	$\sim 10^{70}$	~ 1
10^{22} stars	10^{79}–10^{81}	$\sim 10^7$	10^{63}–10^{65}	10^{-7}–10^{-5}
Stellar black holes	10^{97}–6×10^{97}	$\sim 10^{-7}$	10^{67}–6×10^{67}	10^{-3}–6×10^{-3}
Super massive black holes	10^{102}–3×10^{104}	$\sim 10^{-14}$	10^{65}–3×10^{67}	10^{-5}–3×10^{-3}
Cold dark matter	$\sim 2 \times 10^{88}$	$<10^2$	$<10^{67}$	$<10^{-3}$
CMB photons	10^{88}–2×10^{89}	2.7	3×10^{65}–6×10^{66}	3×10^{-5}–6×10^{-4}
Relic neutrinos	10^{88}–5×10^{89}	2	2×10^{65}–10^{67}	2×10^{-5}–10^{-3}

It is evident from Table 1 that at present, stellar heated gas and dust make up the dominant information energy contribution, as other sources of information energy are miniscule in comparison. The $N \sim 10^{86}$ bits at typical gas and dust temperatures, $T \sim 10^7$, have an equivalent total N k_B T ln(2) energy of $\sim 10^{70}$ J, directly comparable to the $\sim 10^{70}$ J equivalent mc^2 energy of the universe's $\sim 10^{53}$ kg baryons. Stellar heated gas and dust information equivalent energy should then be included alongside the mc^2 equivalence of matter in universe energy accounting. Information energy from stellar heated gas and dust could account for today's dark energy density using accepted physics, relying solely on the experimentally proven Landauer's Principle, combined with realistic entropy estimates, and without invoking any new physics at this stage.

The information energy of stellar heated gas and dust has previously been shown [13,25–27] to provide a near-constant dark energy density in the late universe, effectively emulating a cosmological constant; at earlier times, this dark energy contribution was phantom. The overall time variation—present constant energy density plus earlier phantom—has been shown to be consistent with the Planck-combined datasets [13]. In the next section, we update that previous work by including more recent stellar mass density measurements.

3. Dynamic Information Energy: Time History

In order to include the information energy of stellar heated gas and dust in the accounting of the universe's energy, we need to describe its variation over time by identifying how total bit number, $N(a)$, and typical temperature, $T(a)$, vary as a function of the universe scale size, a, related to redshift, z, by $a = 1/(1 + z)$.

Firstly, we assume that within any sufficiently large volume, the average temperature, $T(a)$, representative of the stellar heated gas and dust, varies in proportion to the fraction, $f(a)$, of baryons that have formed stars up to that scale size. We can determine the history of $f(a)$ by the plotting in Figure 1, a survey of measured stellar mass densities per co-moving volume [28–56] as a function of scale size, a.
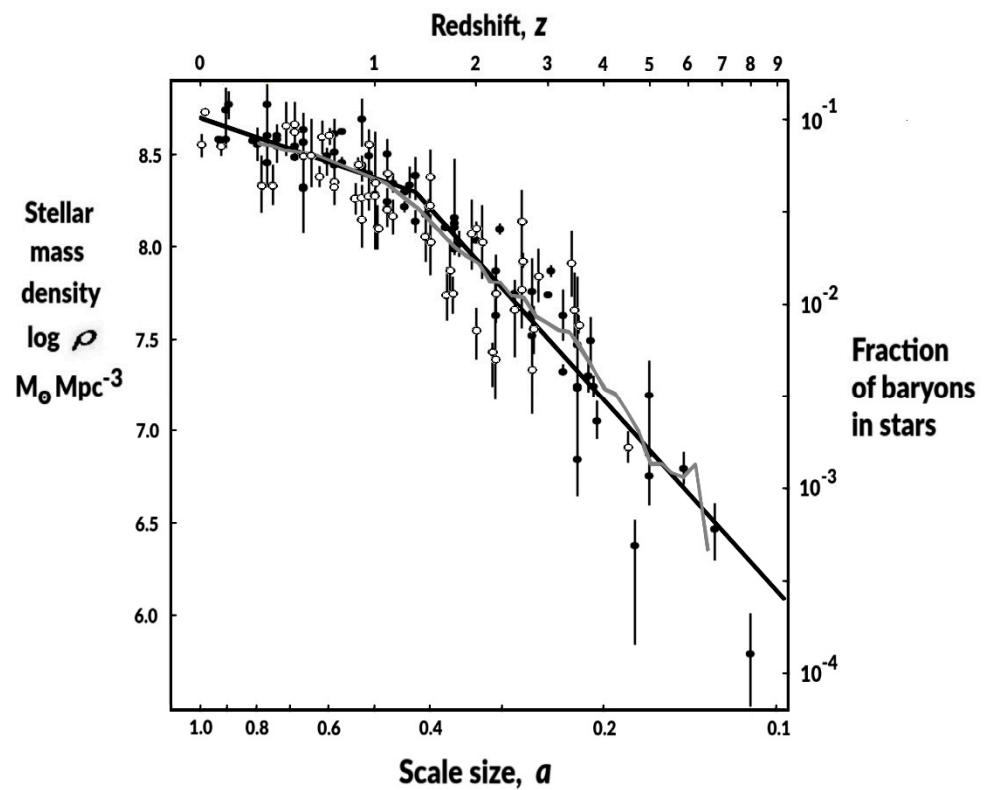
Figure 1. Review of stellar mass density measurements for co-moving volumes as a function of universe scale size, *a*. Straight black lines are power-law fits: $a^{+1.08\pm0.16}$, for $z < 1.35$; and $a^{+3.46\pm0.23}$, for $z > 1.35$. Grey line is the sliding average. Source references: *Filled circles*: [28–44]; *Open circles*: [45–56], see text.

The filled symbols in Figure 1, from source references [28–44], correspond to data compiled for a survey of stellar formation measurements, listed in Table 2 of [57]. A subset of these sources was already used in previous information energy studies [13,26,27], and open symbols, from source references [45–56], correspond to measurements used in those previous studies but were not included in the survey of [57].

In Figure 1, there is a significant change around redshift, $z \sim 1.35$, from a steep gradient in the past to a weaker gradient in recent times. Fitting power laws to data points on either side of $z = 1.35$, we find power laws of $a^{+1.08\pm0.16}$ for $z < 1.35$, and $a^{+3.46\pm0.23}$ for $z > 1.35$. Then, we assume the average stellar heated gas and dust baryon temperature, T, proportional to the fraction of baryons in stars, $f(a)$, also varied as $a^{+1.08\pm0.16}$ for $z < 1.35$, and $a^{+3.46\pm0.23}$ for $z > 1.35$. Measured mean galactic electron temperatures over the range $0 < z < 1$ [58] show a similar temperature time variation as Figure 1, supporting our use of stellar mass densities as a proxy for the gas and dust temperature time variation.

We consider two possibilities for the time variation of total stellar heated gas and the dust bit number, $N(a)$. In the first case, we assume that $N(a)$ simply varies, directly proportional to volume, as a^3. In the second case, we assume that the total bit number of any large co-moving volume is governed by the Holographic Principle [59–61] and varies with the volume's bounding area as a^2. While the Holographic Principle is generally accepted for black holes at the holographic bound, the holographic bound of the universe is $\sim 10^{123}$ bits, and the general principle remains only a conjecture for universal application to cases well below the holographic bound [61].

We wish to compare the time variation of these information energy models against that of the cosmological constant. The Friedmann equation [62] expresses the Hubble parameter, $H(a)$, in terms of its present value, the Hubble constant, H_0, and dimensionless energy density parameters, Ω, expressed as a fraction of today's total energy density. Assuming

that the curvature term is zero, and that the radiation term has for some time been negligible compared to the other terms, the ΛCDM model is described simply by Equation (4).

$$\textbf{ΛCDM: } (H(a)/H_0)^2 = \Omega_{\text{tot}}\, a^{-3} + \Omega_\Lambda \tag{4}$$

for present energy fractional contributions, Ω_{tot} from all matter (dark+baryons), and Ω_Λ from the cosmological constant.

Total information equivalent energy, given by $N\, k_B\, T\, \ln(2)$, is proportional to both $N(a)$ and $T(a)$; it is thus proportional to $a^3\, f(a)$ in the volume model, and proportional to $a^2\, f(a)$ in the holographic model. These correspond to the information energy density terms $\Omega_{\text{IE}}(f(a)/f(1))$ and $\Omega_{\text{IE}}\,(f(a)/f(1))\, a^{-1}$, respectively. Then, if the cosmological constant is negligible and information energy provides the sole source of dark energy, we obtain Equations (5) and (6).

$$\textbf{Information-Volume model: } (H(a)/H_0)^2 = \Omega_{\text{tot}}\, a^{-3} + \Omega_{\text{IE}}\, (f(a)/f(1)) \tag{5}$$

$$\textbf{Information-Holographic model: } (H(a)/H_0)^2 = \Omega_{\text{tot}}\, a^{-3} + \Omega_{\text{IE}}\, (f(a)/f(1))a^{-1} \tag{6}$$

In Figure 2, we compare the effects of these two models for an information energy source of dark energy against the cosmological constant using the present ΛCDM values, setting $\Omega_{\text{tot}} = 0.32$ and $\Omega_\Lambda = \Omega_{\text{IE}} = 0.68$, and applying the power-law fits in Figure 1 for $f(a)$.

We can see from the upper plot of Figure 2 that the total energy density of the holographic model and that of the cosmological constant nearly coincide, while that for the volume model clearly predicts significantly different total energy densities. The lower plot of Figure 2 emphasizes these differences by plotting the percentage difference in the expected Hubble parameter for the information energy models relative to that of the cosmological constant model. The volume model differs significantly from the cosmological constant, peaking at 7% around $a = 0.67$. Such a difference, at $z = 0.5$, from that expected for a cosmological constant should have easily been observed directly by existing expansion measurements, and for this reason, we hereafter concentrate on the holographic model. The holographic model difference is less than 1% for $a > 0.4$ and for $a < 0.2$, peaking at only 1.8% around $a = 0.33$.

The time variation of a dark energy density is proportional to $a^{-3(1+w)}$, where w is the equation of the state parameter for that dark energy. Recently, $z < 1.35$, $T(a)$ varied as $a^{+1.08\pm0.16}$, $N(a)$ as a^{+2}, hence total stellar heated gas and dust information energy varied as $a^{+3.08\pm0.16}$, providing a near-constant energy density varying only as $a^{+0.08\pm0.16}$, corresponding to the equation of the state parameter, $w = -1.03 \pm 0.05$. Then, the information energy of stellar heated gas and dust in the recent period has the characteristics of dark energy, since $f(a)$ closely follows the a^{+1} gradient that would lead to a near-constant information energy density and emulate a cosmological constant, $w = -1$. Thus, information energy can provide a quantitative account of dark energy, accounting for both the present energy value, $\sim 10^{70}$ J, and the recent period of near-constant energy density.

In comparison, during the earlier period, $z > 1.35$, T varied as $a^{+3.46\pm0.23}$, total information energy varied as $a^{+5.46\pm0.23}$, providing a phantom energy with an energy density increasing as $a^{+2.46\pm0.23}$, corresponding to $w = -1.82 \pm 0.08$. The error bars on the equation of the state parameters of both recent and earlier periods are set here by the error bars of the power-law fits in the data of Figure 1. Note that the equation of the state parameter values, $w = -1.03 \pm 0.05\ z < 1.35$ and $w = -1.82 \pm 0.08\ z > 1.35$, are not particularly sensitive to the precise redshift value assumed for the power law break point. For example, choosing break points earlier, $z = 1.55$, or later, $z = 1.15$, the power-law fits to the data of Figure 1 yield very similar values: $w = -1.06 \pm 0.05$, $z < 1.55$; $w = -1.84 \pm 0.09$, $z > 1.55$; $w = -1.00 \pm 0.06$, $z < 1.15$; and $w = -1.79 \pm 0.07$, $z > 1.15$.
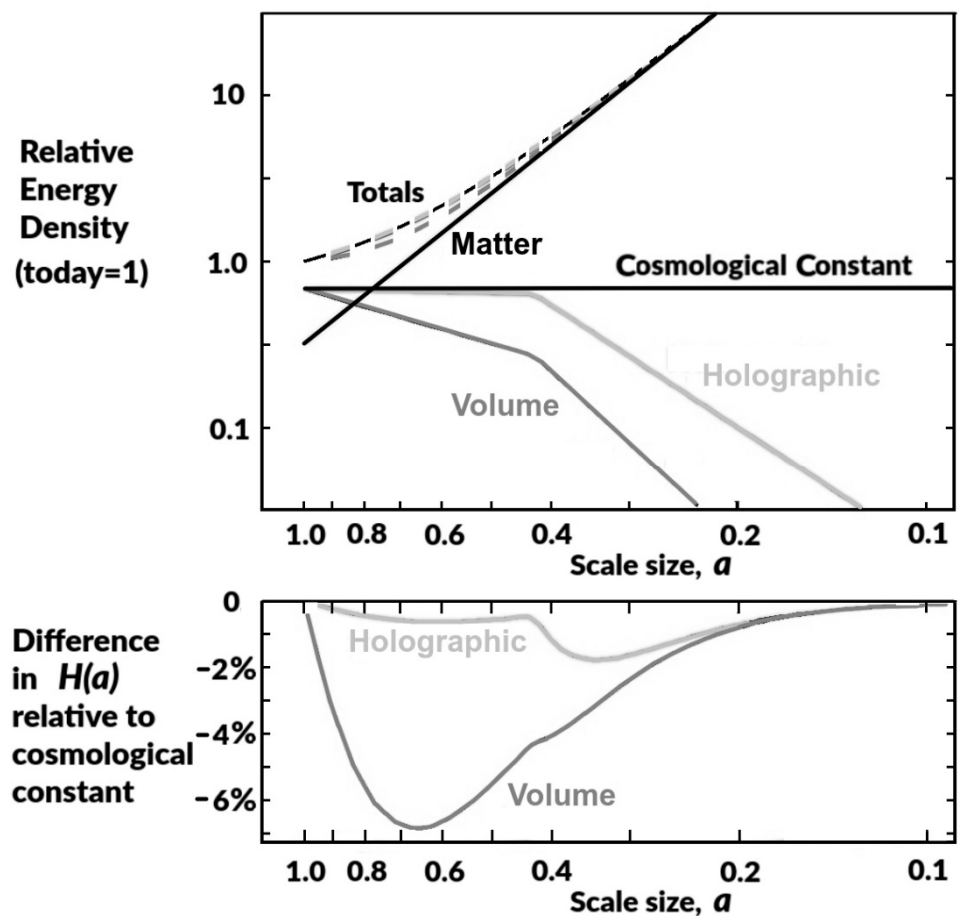
Figure 2. *Upper Plot.* Energy densities relative to total today (=1.0) for the cosmological constant, information energy, and all matter; the plot includes totals (dashed lines) for all matter+cosmological constant, and all matter+information energy, for the volume and holographic models. *Lower Plot.* Difference in the Hubble parameter, *H(a)*, to be expected from an information energy source of dark energy relative to that resulting from a cosmological constant. Both plots assume the power-law fits in Figure 1 data.

4. Information Energy Can Account for H_0 Tension

Results of experiments to measure the dark energy equation of state, w, often assume a simple shape for the $w(a)$ timeline, using a minimum number of parameters. Most astrophysical datasets, including Planck data releases [1,63–65], have been analyzed to deduce cosmological parameters using the Chevalier, Polarski, Linder, CPL description [66]: $w(a) = w_0 + (1 − a)w_a$. This assumes a smooth variation of $w(a)$ from $w_o + w_a$ at very early times, $a \ll 1$, through to w_o today ($a = 1$).

The 2013–2018 Planck data releases include several dataset combinations, where Planck data have been combined with other types of measurement and analyzed using the CPL parameters. Although the resultant likelihood regions of $w_o − w_a$ space always include the cosmological constant, consistent with ΛCDM, there is a clear overall bias towards an early phantom dark energy (Figure 36 of [63], Figure 28 of [64], Figure 30 of [1]). Most of the likelihood area is located in the space where $w_o + w_a < −1$, the phantom shaded area of Figure 30 in [1].

The information energy equation of the state parameter values, $w = −1.03 \pm 0.05$, $z < 1.35$, and $w = −1.82 \pm 0.08$, $z > 1.35$, correspond to the CPL parameters, $w_0 = −1.03 \pm 0.05$, $w_a = −0.79 \pm 0.08$, located close to the center of these maximum likelihood regions in $w_o − w_a$ space. While the volume model would lead to easily identifiable differences from ΛCDM at low z, the holographic model emulates a cosmological constant at low z, and

for most phenomena, it would be indistinguishable from ΛCDM. The difference between the information energy CPL parameters and those for Λ, $w_0 = -1$, $w_a = 0$, is then given by $\Delta w_0 = -0.03 \pm 0.05$ and $\Delta w_a = -0.79 \pm 0.08$. These parameter differences are significant as they closely match the differences previously considered as the possible means by which a dynamic dark energy could account for the H_0 tension. A dynamic dark energy differing from Λ by $\Delta w_0 = -0.08$ and $\Delta w_a = -0.8$ has been shown to be capable of accounting for much of the 'H$_0$ tension', from Figure 4 in [4]. Therefore, information dark energy could quantitatively account for the 'H$_0$ tension'.

Note that CPL parameters fit the information *w(a)* values, both today and very early, but information energy exhibits a much sharper transition at $z\sim1.35$ than can be faithfully described by CPL. Clearly, the best fit would be provided by the simple sharp transition description: $w = w_o = -1.03$ for $z < 1.35$, and $w = w_o + w_a = -1.82$ for $z > 1.35$. At $z > 2$, dark information energy is negligible, less than 3 percent of total matter energy density; however, it increases rapidly to a near-constant energy density by $z\sim1.35$. Such a transitional dark energy, with a sharp change in w in the range of $1 < z < 2$, with a negligible dark energy density at $z > 2$, has previously been shown to be capable of largely accounting for both the 'H$_0$ tension' and also the 'σ_8 tension' between early and late universe values of the matter fluctuation amplitude [67].

5. Information Dark Energy Is Falsifiable by Experiment

The dark energy properties of the information energy identified above might still be just a fortuitous coincidence, and in order to confirm or refute this proposed source of dark energy, we need to predict the value of some future measurement(s).

The main detectable effect of dark energy is the resulting accelerating expansion of the universe. Unfortunately, as information dark energy has closely emulated a cosmological constant in recent times, any differences will be hard to measure. Nevertheless, the clearest verification of information energy's role as the source of dark energy would be provided by measuring the expected small difference in the Hubble parameter from that of the cosmological constant (Figure 2, lower plot). This difference is a direct result of the earlier phantom period of information energy caused by the steeper stellar mass density gradient at $z > \sim1.35$. This small reduction in *H(a)* is bounded at low redshift by the location of the change of gradient in the Figure 1 measurements, and at higher redshift by the much higher matter energy densities swamping any dark energy contribution.

Power laws were used above primarily to facilitate estimates of the equation of state parameters. Now, we wish to avoid the possibility that the expected difference is an artefact of fitting power laws. Accordingly, in Figure 3, we also apply a sliding average of the Figure 1 measurements (Figure 1, grey line) to generate a data-driven *f(a)*, independent of fitted function.
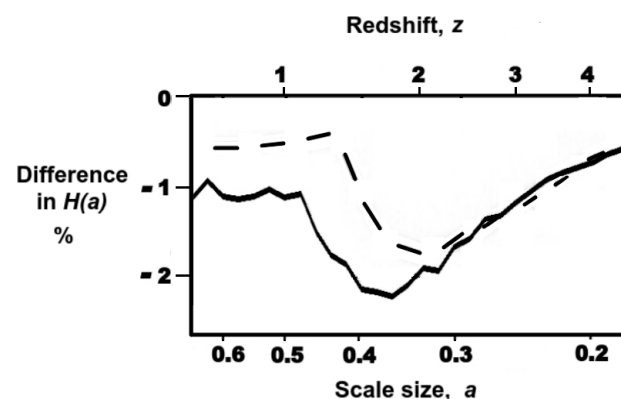
Figure 3. Difference in *H(a)* expected between information energy and the cosmological constant sources of dark energy. Solid black line derived from the sliding average of the data in Figure 1, and dashed line from the power-law fits used previously.

In Figure 3, both methods predict similar values for the signature that would be produced by an information dark energy. The sliding average predicts a maximum difference of -2.2% at $z{\sim}1.7$, while the power-law fits predict a maximum of -1.8% at $z{\sim}2$. There is a clear prediction of a measurable reduction in $H(a)$ relative to the cosmological constant over a specific limited redshift range, and hence constitutes a means by which information dark energy can be falsified experimentally.

6. Discussion

The present information dark energy value, obtained directly from realistic estimates of bit numbers and temperatures, could account for the accelerating expansion. The late time near-constant energy density follows directly from the measured stellar mass density gradient, providing a $T(a)$ variation closely proportional to a^{+1}, combined with the total $N(a)$ proportional to a^{+2}, assuming the general holographic principle. Strong additional support for an information dark energy is provided by its ability to resolve significant problems or tensions that otherwise remain unexplained and incompatible with the standard ΛCDM model:

6.1. H_0 and σ_8 Tensions

In Section 4, we saw that an information dark energy can account for much of the 'H$_0$ tension'. The closest CPL parameter description for information energy is identical to the values suggested by Reiss et al. [4] for a dynamic dark energy explanation. A more appropriate description of information energy, accounting for the sharp transition around $z{\sim}1.35$, is identical to the transitional dark energy model [67] that can account for both the H$_0$ tension and the σ_8 tension.

6.2. Cosmological Constant Problem

Theoretical estimates for a non-zero value of Λ differ by a massive factor of $\sim 10^{120}$ from the actual value required to account for observed accelerating expansion. Despite the lack of any quantitative physical explanation, Λ has been accepted hitherto primarily because of its simplicity and ability to fit the data [68]. Before the expansion of the universe was found to be accelerating, Weinberg [69] considered the most likely value for Λ to be zero. Accounting for all dark energy with information energy would allow Λ to take that preferred zero value, and the information dark energy would effectively resolve the 'cosmological constant problem'.

6.3. Cosmological Coincidence Problem

Star formation needed to have advanced sufficiently for information dark energy to be strong enough to initiate accelerating expansion. Star formation also needed to have advanced sufficiently for there to be a significant likelihood of intelligent beings evolving to observe this acceleration. Therefore, it does not seem to be such a coincidence that we are living when the expansion is accelerating. This effectively removes the 'why now?' of the 'cosmological coincidence problem' (for example, see [70]).

6.4. Cosmic Isotropy

We expect information energy, which is dependent on structure and star formation, to be both temporal and spatially dynamic. Above, we used the universe averaged temporal variation to determine equation of state parameters. Recently, large 5σ significance directional anisotropies have been observed in the value of H_0 [71], calling into question the cosmic isotropy assumption of the cosmological principle. Such directional anisotropies should be expected from the spatial dynamic aspect of an information dark energy located in the stellar heated gas and dust of structures.

6.5. Falsifiable

Note that the predicted $\sim$2% difference in the curve of *H(a)* at *z*$\sim$2, as shown in Figure 3, is close to the detection limit of next generation instruments. For example, the ESA Euclid science requirement document [72] states that the aim is to measure *H(a)* down to an accuracy of 1–2% in the range of $0.5 < z < 2$. Notwithstanding the resolution limits of present instrument designs, this clear prediction will still enable information dark energy to be falsified experimentally in the near future.

Instead of waiting for sufficiently high-resolution measurements of *H(a)* to become available, another method of verifying the role of information dark energy would be to determine whether the observed directional anisotropies in H_0 [71] are related to the distribution of stellar heated gas and dust in the structures of the universe.

6.6. Information Dark Energy Compared to Λ and Quintessence

In the discussions above, we have shown that information energy in the late universe closely mimics a cosmological constant. Information energy, IE, can just replace Λ in the ΛCDM model, effectively creating an IECDM model. Then, as the only observable effect of dark energy is via the accelerating expansion, this model should be as consistent with other phenomena as ΛCDM, while also resolving the H_0 and σ_8 tensions, the cosmological constant and cosmological coincidence problems, and removing the cosmic isotropy assumption of ΛCDM.

Table 2 summarizes and shows that information dark energy compares favourably against the two main dark energy theories: the cosmological constant and scalar fields/quintessence.

Table 2. Comparison of information energy to two main dark energy theories.

Dark Energy Property Required to Fit Observations	Cosmological Constant	Scalar Fields/ Quintessence	Information Energy
Account quantitatively for present dark energy value	Not by orders of magnitude	Only by much fine tuning	Yes, directly $\sim 10^{70}$ J
Resolve 'Cosmological constant problem'	No	Only by much fine tuning	Yes $\Lambda \rightarrow 0$
Late universe near-constant dark energy density, $w \sim -1$	Yes, by definition, $w = -1$	Not specific $-1 < w < +1$	Yes $w = -1.03 \pm 0.05$
Consistent with *Planck* $w_0 - w_a$ parameter likelihood region	Yes	Not specific	Yes
Resolve late vs. early universe 'H_0 and σ_8 tensions'	No	No	Yes, quantitatively
Resolve 'Cosmic coincidence problem'	No	Only by much fine tuning	Yes, naturally
Account for H_0 anisotropies that conflict with 'cosmic isotropy'	No	No	Yes, expected
Experimentally Falsifiable?	No	No	Yes, Predicted *H(a)*

Table 2 shows that the equivalent energy of the information/entropy associated with stellar heated gas and dust has many of the characteristics required to be the source of dark energy. In our modified Friedmann Equations (5) and (6), this energy equivalence of information is used in the same way as, and alongside, the mc^2 energy equivalence of matter. We have not needed to identify specific processes nor required information to be destroyed any more than matter needs to be destroyed in order to consider these equivalent energies.

If information dark energy is indeed found to account for the accelerating expansion, then three further aspects should also be considered:

6.7. Constant Information Energy Density from Feedback?

The advent of accelerating expansion has been associated with directly causing a general reduction in galaxy merging and a reduction in the growth rate of structure and the rate of star formation [73,74]. This effect is evident in Figure 1 in the clear change of the stellar mass density gradient at *z*$\sim$1.35, from $a^{+3.46 \pm 0.23}$ to $a^{+1.08 \pm 0.16}$, coincident

with the start of dark energy acceleration effects. Assuming dark energy is information energy, once the information energy density, which increased with star formation, was strong enough to initiate acceleration, the acceleration in turn slowed down star formation, acting as a feedback that directly limited the growth rate of information energy itself. The resulting $a^{+1.08\pm0.16}$ gradient that we observe in Figure 1 is then significant as this range encompasses the specific gradient of a^{+1}, which should be the natural feedback limited stable value expected from our information energy explanation for dark energy. The constant information energy density at $z < 1.35$, mimicking a cosmological constant, is then a direct result of this feedback limiting. Moreover, in order for feedback to operate in this way, information energy would need to be the major, or sole, source of dark energy.

6.8. Can Information Energy Also Emulate Dark Matter Effects?

In this work, we have concentrated on considering the dark energy aspects of information energy. However, another aspect that should be considered is that information energy might contribute to some effects previously attributed to dark matter. We have shown that information energy from stellar heated gas, primarily located around structures, has an energy density at a similar order of magnitude to total matter. Now space-time will be equally distorted by accumulations of matter and equivalent accumulations of energy. Then, information energy will distort space-time, adding to some extent a local attractive force emulating that of gravity from an unseen mass. While on the scale of the universe, total information energy as a dark energy is effectively repulsive thus causing the expansion to accelerate, any extra local distortions to space-time around structures caused by information energy will be effectively attractive and mimic dark matter. Then, by the nature and location of information energy in stellar heated gas and dust, it will be hard to distinguish such effects from those usually attributed to dark matter.

A high correlation has been found in [75,76], showing that dark matter effects in a range of galaxies are fully specified by the location of the baryons. This observation is considered difficult to reconcile with ΛCDM, and the Modified Newtonian Dynamics, MOND, has been suggested as a possible explanation. Equally, this observation might be explained by the information energy of stellar heated gas and dust, contributing effects similar to those produced by dark matter. The strongest dark matter effects in clusters of galaxies are found in the brightest and therefore highest-temperature galaxy [77], again consistent with the highest information energy densities located where stellar heated gas and dust occur at high temperatures and densities.

Clusters of colliding galaxies are often considered to provide some of the strongest evidence for the existence of dark matter. Optical observations show stars pass through the collision largely unhindered, whereas X-ray observations show the galactic gas clouds colliding, slowing down, or even halting. The location of dark matter is then identified from the use of lensing measurements [78–80]. A study of the Bullet cluster, and of a further 72 mergers, both major and minor, finds no evidence for dark matter deceleration, with the dark mass remaining closely co-located with the stars and structure. Information energy could equally explain these effects attributed to dark matter, as information energy from stellar heated gas and dust passes, along with the stars, straight through the collision of galaxies. Any contribution of information energy to dark matter effects could be determined by identifying whether the location of the stellar heated gas and dust within galaxies is related to the distribution of dark matter effects observed within those galaxies. New weak-lensing measurements of galaxies [81] promise to measure such effects and distinguish between the various proposed causes.

6.9. A Different Future?

The ΛCDM model assumes that universe expansion will continue accelerating forever in this dark energy-dominated epoch. A dark energy provided by the information energy of stellar heated gas and dust suggests a different future for the universe. The fraction of baryons in stars must stop increasing at some time, since $f(a) < 1$ by definition. Eventually,

f(a) will decrease as more stars die out than new ones are formed. It is estimated that the future maximum star formation might be as little as only 5% higher than today [82]. At some point, the information dark energy density will fall, and the expansion of the universe will cease accelerating and revert back to deceleration.

7. Summary

The approach employed in this work has emphasized the two preferred requirements of cosmology [68]: simplicity (wielding Occam's razor), and naturalness (relying on mostly proven physics, with a strong dependence on empirical data). The information energy of stellar heated gas and dust could provide a dynamic dark energy that overcomes several of the problems and tensions of ΛCDM. It is therefore important to consider performing the falsification measurements suggested above so that such a simple concept can be confirmed, or refuted.

Conflicts of Interest: The author declares no conflict of interest.

References

1. Plank, C.; Aghanim, N.; Akrami, Y.; Ashdown, M.; Aumont, J.; Baccigalupi, C.; Ballardini, M.; Bnaday, A.J.; Barreiro, R.B.; Bartolo, N.; et al. Planck 2018 results. VI, Cosmological Parameters. *Astron. Astrophys.* **2020**, *641*, A6.
2. Choi, S.K.; Hasselfield, M.; Patty Ho, S.-P.; Koopman, B.; Lungu, M.; Abitboi, M.H.; Addison, G.E.; Ade, P.A.R.; Aiola, S.; Alonso, D.; et al. The Atacama Cosmology Telescope: A measurement of the cosmic microwave power spectra at 98 and 150 GHz. *J. Cosmol. Astropart. Phys.* **2020**, *12*, 045. [CrossRef]
3. Abbott, T.M.C.; Abdalla, F.B.; Annis, J.; Bechtol, K.; Blazek, J.; Benson, B.A.; Bernstein, R.A.; Bernstein, G.M.; Bertin, E.; Brooks, D.; et al. Dark Energy Survey year 1 results: A precise H0 measurement from DES, Bao, D/H data. *Mon. Not. R. Astron. Soc.* **2018**, *480*, 3879. [CrossRef]
4. Reiss, A.G.; Casertano, S.; Yuan, W.; Macri, L.M.; Scolnic, D. Large Magellanic Cloud Cepheid Standards provide a 1% foundation for determination of H_0 and strong evidence for physics beyond ΛCDM. *Astrophys. J.* **2019**, *876*, 85. [CrossRef]
5. Reiss, A.G.; Casertano, S.; Yuan, W.; Bowers, J.B.; Macri, L.M.; Zinn, J.C.; Scolnic, D. Cosmic distances calibrated to 1% precision with GAIA EDR3 parallaxes and Hubble Space Telescope photometry of 75 Milky Way Cepheids confirm tension with ΛCDM. *Astrophys. J.* **2021**, *908*, L6. [CrossRef]
6. Reiss, A.G.; Yuan, W.; Macri, L.M.; Scolnic, D.; Brout, D.; Casertano, S.; Jones, D.O.; Murakami, Y.; Breuval, L.; Brink, T.G.; et al. A Comprehensive Measurement of the Local Value of the Hubble Constant with 1 km/s/Mpc Uncertainty from the Hubble Space Telescope and the SH0ES Team. *arXiv* **2021**, arXiv:2112.04510.
7. Wong, K.C.; Suyu, S.H.; Chen, G.C.-F.; Rusu, C.E.; Millon, M.; Sluse, D.; Bonvin, V.; Fassnacht, C.D.; Taubenberger, S.; Auger, M.W.; et al. H0LiCOW-XIII. A 2.4% measurement of H0 from lensed quasars: Tension between early- and late-Universe probes. *Mon. Not. R. Astron. Soc.* **2020**, *498*, 1420. [CrossRef]
8. Pesce, D.W.; Braatz, J.A.; Reid, M.J.; Riess, A.G.; Scolnic, D.; Condon, J.J.; Gao, F.; Henkel, C.; Impellizzeri, C.M.V.; Kuo, C.Y.; et al. The megamaser Cosmology Project. XIII. Combined Hubble constant constraints. *Astrophys. J.* **2020**, *891*, L1. [CrossRef]
9. Blakeslee, J.P.; Jensen, J.B.; Chung-Pei Ma Milne, P.A.; Greene, J.E. The Hubble Constant from Infrared surface brightness fluctuation distances. *Astrophys. J.* **2021**, *911*, 65. [CrossRef]
10. Bernal, J.L.; Peacock, A. Conservative Cosmology: Combining data with allowances for unknown systematics. *J. Cosmol. Astropart. Phys.* **2018**, *7*, 002. [CrossRef]
11. Verde, L.; Treu, T.; Riess, A.G. Institute for Theoretical Physics Workshop Meeting Report: Tensions between the early and late Universe. *Nat. Astron.* **2019**, *3*, 891. [CrossRef]
12. Di Valentino, E.; Mena, O.; Pan, S.; Visinelli, L.; Yang, W.; Melchiorri, A.; Mota, D.F.; Riess, A.G.; Silk, J. In the Realm of the Hubble tension, a Review of Solutions. *Class. Quantum Gravity* **2021**, *38*, 153001. [CrossRef]
13. Gough, M.P. A Dynamic Dark Information Energy Consistent with Planck Data. *Entropy* **2014**, *16*, 1902. [CrossRef]
14. Landauer, R. Irreversibility and heat generation in the computing process. *IBM J. Res. Dev.* **1961**, *3*, 183. [CrossRef]
15. Landauer, R. Information is physical. *Phys. Today* **1991**, *44*, 23. [CrossRef]
16. Toyabe, S.; Sagawa, T.; Ueda, M.; Muneyuki, E.; Sano, M. Experimental demonstration of information-to-energy conversion and validation of the generalized Jarzynski equality. *Nat. Phys.* **2010**, *6*, 988. [CrossRef]
17. Berut, A.; Arakelyan, A.; Petrosyan, A.; Ciliberto, A.; Dillenschneider, R.; Lutz, E. Experimental verification of Landauer's principle linking information and thermodynamics. *Nature* **2012**, *483*, 187. [CrossRef]

18. Jun, Y.; Gavrilov, M.; Bechhoefer, J. High-Precision Test of Landauer's Principle in a Feedback Trap. *Phys. Rev. Let.* **2014**, *113*, 190601. [CrossRef]

19. Yan, L.I.; Xiong, T.P.; Rehan, K.; Zhou, F.; Liang, D.F.; Chen, L.; Zhang, J.Q.; Yang, W.L.; Ma, Z.H.; Feng, M. Single Atom Demonstration of the Quantum Landauer Principle. *Phys. Rev. Lett.* **2018**, *120*, 210601. [CrossRef]

20. Zeilinger, A. A Foundational Principle of Quantum Mechanics. *Found. Phys.* **1999**, *29*, 631. [CrossRef]

21. Gough, M.P.; Carozzi, T.; Buckley, A.M. On the similarity of Information Energy to Dark Energy. *arXiv* **2006**, arXiv:Astro-ph/0603084. [CrossRef]

22. Peebles, P.J.E. *Principles of Physical Cosmology*; Princeton University Press: Princeton, NJ, USA, 1993.

23. Frampton, P.H.; Hsu, S.D.H.; Kephart, T.W.; Reeb, D. What is the entropy of the universe? *Class. Quantum Gravity* **2009**, *26*, 145005. [CrossRef]

24. Egan, C.A.; Lineweaver, C.H. A larger estimate of the entropy of the universe. *Astrophys. J.* **2010**, *710*, 1825. [CrossRef]

25. Gough, M.P. Information Equation of State. *Entropy* **2008**, *10*, 150. [CrossRef]

26. Gough, M.P. Holographic Dark Information Energy. *Entropy* **2011**, *13*, 924. [CrossRef]

27. Gough, M.P. Holographic Dark Information Energy: Predicted Dark Energy Measurement. *Entropy* **2013**, *15*, 1133. [CrossRef]

28. Li, C.; White, S.D.M. The distribution of stellar mass in the low-redshift universe. *Mon. Not. R. Astron. Soc.* **2009**, *398*, 2177. [CrossRef]

29. Gallazzi, A.; Brinchmann, J.; Charlot, S.; White, S.D.M. A census of metals and baryons in stars in the local universe. *Mon. Not. R. Astron. Soc.* **2008**, *383*, 1439. [CrossRef]

30. Moustakas, J.; Coil, A.L.; Aird, J.; Blanton, M.R.; Cool, R.J.; Eisenstein, D.J.; Mendez, A.J.; Wong, K.C.; Zhu, G.; Arnouts, S. PRIMUS: Constraints on star formation quenching and Galaxy merging and the evolution of the stellar mass function from z = 0–1. *Astrophys. J.* **2013**, *767*, 50. [CrossRef]

31. Bielby, R.; Hudelot, P.; McCraken, H.J.; Ilbert, O.; Daddi, E.; Le Fevre, O.; Gonzalez-Perez, V.; Kneib, J.-P.; Marmo, C.; Mellier, Y.; et al. The WIRCam Deep Survey-I. Counts, colours, and mass-functions derived from near-infrared imaging in the CFHTLS deep fields. *Astron. Astrophys.* **2012**, *545*, A23. [CrossRef]

32. Perez-Gonzalez, P.G.; Rieke, G.H.; Villar, V.; Barro, G.; Blaylock, M.; Egami, E.; Gallego, J.; Gil de Paz, A.; Pascual, S.; Zamorano, J.; et al. The stellar mass assembly of galaxies from z = 0–4: Analysis of a sample selected in the rest-frame near infrared with Spitzer. *Astrophys. J.* **2008**, *675*, 234. [CrossRef]

33. Ilbert, O.; McCraken, H.J.; LeFevre, O.; Capak, P.; Dunlop, J.; Karim, A.; Renzini, M.A.; Caputi, K.; Boissier, S.; Arnouts, S.; et al. Mass assembly in quiescent and star-forming Galaxies since z > 4 from UltraVISTA. *Astron. Astrophys.* **2013**, *556*, A55. [CrossRef]

34. Muzzin, A.; Marchesini, D.; Stefanon, S.; Franx, M.; McCraken, H.J.; Milvang-Jensen, B.; Dunlop, J.S.; Fynbo, J.P.U.; Brammer, G.; Labbe, I.; et al. The evolution of the stellar mass functions of star-forming and quiescent galaxies to z = 4 from the COSMOS/UltraVISTA survey. *Astrophys. J.* **2013**, *777*, 18. [CrossRef]

35. Arnouts, S.; Walcher, C.J.; LeFevre, O.; Zamorani, G.; Ilbert, O.; LeBrun, V.; Pozzetti, L.; Bardelli, S.; Tresse, L.; Zucca, E.; et al. The SWIRE-VVDS-CFHTLS surveys: Stellar Assembly over the last 10 Gyr. *Astron. Astrophys.* **2007**, *476*, 137. [CrossRef]

36. Pozzetti, L.; Bolzonella, M.; Zucca, E.; Zamorani, G.; Lilly, S.; Renzini, A.; Moresco, M.; Mignoli, M.; Cassata, P.; Tasca, L.; et al. zCOSMOS-10 k bright spectroscopic sample. The bimodality in the galaxy stellar mass function. *Astron. Astrophys.* **2010**, *523*, A13. [CrossRef]

37. Kajisawa, M.; Ichikawa, T.; Tanaka, I.; Konishi, M.; Yamada, T.; Akiyama, M.; Suzuki, R.; Tokoku, C.; Uchimoto, Y.K.; Yoshikawa, T.; et al. MOIRCS deep survey IV evolution of galaxy stellar mass function back to z~3. *Astrophys. J.* **2009**, *702*, 1393. [CrossRef]

38. Marchesini, D.; van Dokkum, P.G.; Forster Schreiber, N.M.; Franx, M.; Labbe, I.; Wuyts, S. The evolution of the stellar mass function of galaxies from z = 4 and the first comprehensive analysis of its uncertainties. *Astrophys. J.* **2009**, *701*, 1765. [CrossRef]

39. Reddy, N.A.; Dickinson, M.; Elbaz, D.; Morrison, G.; Giavalisco, M.; Ivison, R.; Papovich, C.; Scott, D.; Buat, V.; Burgarella, D.; et al. GOODS-HERSCHEL measurements of the dust attenuation of typical star forming galaxies at high redshift. *Astrophys. J.* **2012**, *744*, 154. [CrossRef]

40. Caputi, K.J.; Cirasuolo, M.; Jdunlop, J.S.; McLure, R.J.; Farrah, D.; Almaini, O. The stellar mass function of the most massive Galaxies at 3 < z < 5 in the UKIDSS Ultra Deep Survey. *Mon. Not. R. Astron. Soc.* **2011**, *413*, 162.

41. Gonzalez, V.; Labbe, I.; Bouwens, R.J.; Illingworth, G.; Frank, M.; Kriek, M. Evolution of galaxy stellar mass functions, mass densities, and mass-to light ratios from z~7 to z~4. *Astrophys. J.* **2011**, *735*, L34. [CrossRef]

42. Lee, K.S.; Ferguson, H.C.; Wiklind, T.; Dahlen, T.; Dikinson, M.E.; Giavalisco, M.; Grogin, N.; Papovich, C.; Messias, H.; Guo, Y.; et al. How do star-forming galaxies at z > 3 assemble their masses? *Astrophys. J.* **2012**, *752*, 66. [CrossRef]

43. Yabe, K.; Ohta, K.; Iwata, I.; Sawicki, M.; Tamura, N.; Akiyama, M.; Aoki, K. The stellar populations of Lyman break galaxies at z~5. *Astrophys. J.* **2009**, *693*, 507. [CrossRef]

44. Labbe, I.; Oesch, P.A.; Bouwens, R.J.; Illingworth, G.D.; Magee, D.; Gonzalez, V.; Carollo, C.M.; Franx, M.; Trenti, M.; van Dokkkum, P.G.; et al. The spectral energy distributions of z = 8 galaxies from the IRAC ultra deep fields. *Astrophys. J.* **2013**, *777*, L19. [CrossRef]

45. Cole, S.; Norberg, P.; Baugh, C.M.; Frenk, C.S.; Bland-Hawthorn, J.; Bridges, T.; Cannon, R.; Colless, M.; Collins, C.; Couch, W.; et al. The 2dF galaxy redshift survey. *Mon. Not. R. Astron. Soc.* **2001**, *326*, 255. [CrossRef]

46. Dickinson, M.; Papovich, C.; Ferguson, H.C.; Budavari, T. The evolution of the global stellar mass density a 0 < z < 3. *Astrophys. J.* **2003**, *587*, 25.
47. Rudnick, G.; Rix, H.-W.; Franx, M.; Labbe, I.; Blanton, M.; Daddi, E.; Forster-Schreiber, N.M.; Moorwood, A.; Rottgering, H.; Trujillo, I.; et al. The rest-frame optical luminosity density, colour, and stellar mass density of the universe from z = 0 to z = 3. *Astrophys. J.* **2003**, *599*, 847. [CrossRef]
48. Brinchmann, J.; Ellis, R.S. The mass assembly and star formation characteristics of field galaxies of known morphology. *Astrophys. J.* **2000**, *536*, L77. [CrossRef]
49. Elsner, F.; Feulner, G.; Hopp, U. The impact of Spitzer infrared data on stellar mass estimates. *Astron. Astrophys.* **2008**, *477*, 503. [CrossRef]
50. Drory, N.; Salvato, M.; Gabasch, A.; Bender, R.; Hopp, U.; Feuler, G.; Pannella, M. The stellar mass function of galxies to z~5. *Astrophys. J.* **2005**, *619*, L131. [CrossRef]
51. Drory, N.; Alvarez, M. The contribution of star formation and merging to stellar mass buildup in galaxies. *Astrophys. J.* **2008**, *680*, 41. [CrossRef]
52. Fontana, A.; Donnarumma, I.; Vanzella, E.; Giallongo, E.; Menci, N.; Nonimo, M.; Saracco, P.; Cristiani, S.; D'Odorico, S.; Poli, F. The assembly of massive galaxies from near Infrared observations of Hubble deep-field south. *Astrophys. J.* **2003**, *594*, L9. [CrossRef]
53. Fontana, A.; Salimeni, S.; Grazian, A.; Giallongo, E.; Pentericci, L.; Nonino, M.; Fontanot, F.; Menci, N.; Monaco, P.; Cristiani, S.; et al. The galaxy mass function up to z = 4 in the GOODS-MUSIC sample. *Astron. Astrophys.* **2006**, *459*, 745. [CrossRef]
54. Cohen, J.G. CALTECH faint galaxy redshift survey. *Astrophys. J.* **2002**, *567*, 672. [CrossRef]
55. Conselice, C.J.; Blackburne, J.A.; Papovich, C. The luminosity, stellar mass, and number density evolution of field galaxies. *Astrophys. J.* **2005**, *620*, 564. [CrossRef]
56. Borch, A.; Meisenheimer, K.; Bell, E.F.; Rix, H.-W.; Wolf, C.; Dye, S.; Kleinheinrich, M.; Kovacs, Z.; Wisotzki, L. The stellar masses of 25,000 galaxies at 0.2 < z < 1.0 estimated by COMBO-17 survey. *Astron. Astrophys.* **2006**, *453*, 869.
57. Madau, P.; Dickinson, M. Cosmic Star Formation History. *Ann. Rev. Astron. Astrophys.* **2014**, *52*, 415. [CrossRef]
58. Chiang, Y.-K.; Makiya, R.; Menard, B.; Komatsu, E. The Cosmic Thermal History Probed by Sunyaev Zeldovich Effect Tomography. *Astrophys. J.* **2020**, *902*, 56. [CrossRef]
59. T'Hooft, G. Obstacles on the way towards the quantization of space, time and matter- and possible solutions. *Stud. Hist. Philos. Mod. Phys.* **2001**, *32*, 157. [CrossRef]
60. Susskind, L. The world as a hologram. *J. Math. Phys.* **1995**, *36*, 6377. [CrossRef]
61. Buosso, R. The holographic principle. *Rev. Mod. Phys.* **2002**, *74*, 825. [CrossRef]
62. Friedmann, A. On the Curvature of Space. *Gen. Relativ. Gravit.* **1999**, *31*, 1991. [CrossRef]
63. Ade, P.; Aghanim, N.; Armitage-Caplan, C.; Arnaud, M.; Ashdown, M.; Atrio-Barandela, F.; Aumont, J.; Baccigalupi, C.; Banday, A.J.; Barreiro, R.B.; et al. Plank Collaboration. Planck 2013 results. XVI. Cosmological parameters. *Astron. Astrophys.* **2014**, *571*, A16.
64. Ade, P.; Aghanim, N.; Arnaud, M.; Ashdown, M.; Aumont, J.; Baccigalupi, C.; Banday, A.J.; Barreiro, R.B.; Bartlett, J.G.; Bartolo, N.; et al. Plank Collaboration. Planck 2015 results. XIII. Cosmological parameters. *Astron. Astrophys.* **2016**, *594*, A13.
65. Ade, P.; Aghanim, N.; Arnaud, M.; Ashdown, M.; Aumont, J.; Baccigalipi, C.; Banday, A.J.; Barreiro, R.B.; Bartolo, N.; Battaner, E.; et al. Planck Collaboration. Planck 2015 results. XIV. Dark energy and modified gravity. *Astron. Astrophys.* **2016**, *594*, A14.
66. Chevallier, M.; Polarski, D. Accelerating universes with scaling dark matter. *Int. J. Mod. Phys.* **2001**, *D10*, 213. [CrossRef]
67. Keeley, R.; Joudaki, S.; Kaplinghat, M.; Kirkby, D. Implications of a transition in the dark energy equation of state for the H0 and σ8 tensions. *J. Cosmol. Astropart. Phys.* **2019**, *12*, 035. [CrossRef]
68. Bull, P.; Akrami, Y.; Adamek, J.; Baker, T.; Bellini, E.; Beltran-Jimenez, J.; Bentivegna, E.; Camera, S.; Clesse, S.; Davis, J.H.; et al. Beyond ΛCDM: Problems, solutions, and the road ahead. *Phys. Dark Universe* **2016**, *12*, 56. [CrossRef]
69. Weinberg, S. The cosmological constant problem. *Rev. Mod. Phys.* **1989**, *61*, 1. [CrossRef]
70. Velten, H.G.; vom Marttens, R.F.; Zimdahi, W. Aspects of the cosmological coincidence problem. *Eur. Phys. J. C* **2014**, *74*, 3160. [CrossRef]
71. Migkas, K.; Schellenberger, G.; Reiprich, T.H.; Pacaud, F.; Ramos-ceja, M.E.; Lovisari, L. Probing cosmic isotropy with a new X-ray galaxy cluster sample through the Lx -T scaling relation. *Astron. Astrophys.* **2020**, *636*, A15. [CrossRef]
72. ESA Euclid Science Requirements Document. Available online: https://sci.esa.int/web/euclid/-/42822-scird-for-euclid (accessed on 27 July 2021).
73. Guzzo, L.; Pierleoni, M.; Meneux, B.; Branchini, E.; LeFevre, O.; Marinoni, C.; Garilli, B.; Blaizot, J.; DeLucia, G.; Pollo, A.; et al. A test of the nature of cosmic acceleration using galaxy redshift distortions. *Nature* **2008**, *451*, 541. [CrossRef] [PubMed]
74. Frieman, J.A.; Turner, M.S.; Huterer, D. Dark energy and the accelerating universe. *Ann. Rev. Astron. Astrophys.* **2008**, *46*, 385. [CrossRef]
75. McGaugh, S.S.; Lelli, F.; Schombert, J.M. The Radial Acceleration Relation in Rotationally Supported Galaxies. *Phys. Rev. Lett.* **2016**, *117*, 201101. [CrossRef] [PubMed]

76. Lelli, F.; McGaugh, S.S.; Schombert, J.M.; Pawlowski, M.S. One Law to Rule them all: The Radial Acceleration relation of Galaxies. *Astrophys. J.* **2017**, *836*, 152. [CrossRef]

77. Viola, M.; Cacciato, M.; Brouwer, M.; Kuijken, K.; Hoekstra, H.; Norberg, P.; Robotham, A.S.G.; van Uitert, E.; Alpasian, M.; Baldry, I.K.; et al. Dark matter halo properties of GAMA galaxy groups from 100 square degrees of KiDS weak lensing data. *Mon. Not. R. Astron. Soc.* **2015**, *452*, 3529. [CrossRef]

78. Markevich, M.; Gonzalez, A.H.; Clowe, D.; Vikhlinin, A.; Forman, W.; Jones, C.; Murray, S.; Tucker, W. Direct constraints on the dark matter self-interaction cross-section from the merging galaxy cluster. *Astrophys. J.* **2004**, *606*, 819. [CrossRef]

79. Harvey, D.; Massey, R.; Kitching, T.; Taylor, A.; Tittley, E. The non gravitational interactions of dark matter in colliding galaxy clusters. *Science* **2015**, *347*, 1462. [CrossRef]

80. Massey, R.; Williams, L.; Smit, R.; Swinbank, M.; Kitching, T.D.; Harvey, D.; Jauzac, M.; Israel, H.; Clowe, D.; Edge, A.; et al. The behaviour of dark matter associated with four bright Cluster galaxies in the 10 kpc core of Abell 3827. *Mon. Not. R. Astron. Soc.* **2015**, *449*, 3393. [CrossRef]

81. Brouwer, M.M.; Oman, K.A.; Valentijn, E.A.; Bilicki, M.J.; Heymans, C.; Hoekstra, H.; Napolitano, N.R.; Roy, N.; Tortora, C.; Wright, A.H.; et al. The weak lensing radial acceleration relation: Constraining modified gravity and cold dark matter theories. *Astron. Astrophys.* **2021**, *650*, A113. [CrossRef]

82. Sobral, D.; Small, I.; Best, P.N.; Geach, J.E.; Yuichi, M.; Stott, J.P.; Cirasuolo, M.; Jaron, K. A large Hα survey at z = 2.23, 1.47, 0.84 and 0.40: The 11 Gyr evolution of star-forming galaxies from HiZELS. *Mon. Not. R. Astron. Soc.* **2013**, *428*, 1128. [CrossRef]